

Dual-functional CeO_x fence promoting Au nanocatalyst for CO oxidation under wide working conditions

Jie Chen^{a,b,c,*}, Jianhui Huang^{d,*}, Jianpeng Zeng^a, Fengying Zheng^{a,b,c}, Shunxing Li^{a,b,c,*}

a College of Chemistry, Chemical Engineering and Environment, Minnan Normal University, Zhangzhou 363000, China

b Fujian Province Key Laboratory of Modern Analytical Science and Separation Technology, Minnan Normal University, Zhangzhou 363000, China

c Fujian Province University Key Laboratory of Pollution Monitoring and Control, Minnan Normal University, Zhangzhou 363000, China

d College of Rare Earths, Jiangxi University of Science and Technology, Ganzhou, 341000, China

* Corresponding authors: chenj@mnnu.edu.cn; shunxing_li@aliyun.com; huangjianhui@jxust.edu.cn

Experimental Section

Materials and reagents

The chemicals including $\text{Ce}(\text{NO}_3)_3 \cdot 6\text{H}_2\text{O}$, NaOH, rutile TiO_2 support, Fe_2O_3 support and ZrO_2 support were purchased from Aladdin Shanghai Co., Ltd. HAuCl_4 were bought from Sinopharm Chemical Reagent Co., Ltd. All the reagents used were analytical grade in purity. Ultrapure water (Millipore Milli-Q grade) with a resistivity of $18.2 \text{ M}\Omega$ was used in all the experiments. The commercial Au/ TiO_2 catalyst was purchased from Strem Chemicals.

Catalyst preparation

Preparation of Au@1Ce-RTi and Au@5Ce-RTi catalysts. 1 g of support (rutile TiO_2) was dispersed in 50 mL of water by sonication treatment for 30 min. Then 1 mL of $\text{Ce}(\text{NO}_3)_3$ aqueous solution (0.05 M) was added under stirring, followed by addition of 1 mL of NaOH aqueous solution (0.15 M). After 1 min vigorous stirring, 1 mL of HAuCl_4 solution (0.01 g mL^{-1}) was added dropwise and stirring for another 30 min. The precipitate was collected and washed with deionized water several times, followed by drying at $80 \text{ }^\circ\text{C}$ overnight. Finally, the powder was calcined at $400 \text{ }^\circ\text{C}$ for 2 h at a heating rate of $2 \text{ }^\circ\text{C min}^{-1}$ under air condition. After calcination, the as-prepared catalyst was collected and named as Au@1Ce-RTi catalyst. For Au@5Ce-RTi catalyst, 1 mL of $\text{Ce}(\text{NO}_3)_3$ aqueous solution (0.25 M) was added under stirring, followed by addition of 1 mL of NaOH aqueous solution (0.75 M).

Preparation of Au-RTi catalyst. This catalyst was prepared by the conventional impregnation method. 1 g of rutile TiO_2 support was immersed in 10 mL of HAuCl_4 solution containing 0.01 g of Au element. The water was fully evaporated from the mixture at $80 \text{ }^\circ\text{C}$ for overnight, and then the powder was calcined at $400 \text{ }^\circ\text{C}$ for 2 h at a heating rate of $2 \text{ }^\circ\text{C min}^{-1}$ under air condition.

Preparation of Au@3Ce-Zr and Au@3Ce-Fe catalysts. The catalysts were prepared by the same method like Au@3Ce-RTi catalyst except that the support was changed to ZrO_2 and Fe_2O_3 .

Catalyst characterization

The Au content was determined using inductively coupled plasma optical emission spectrometry (ICP-OES) with a Aglient 7800.

Powder X-ray diffraction (XRD) data was collected on a Bruker AXS D2 ADVANCE diffractometer using Cu K α radiation ($\lambda = 1.5418 \text{ \AA}$). The scan range was 5-90° while the step size was 0.02°.

Transmission electron microscopy (TEM) and high-resolution transmission electron microscopy (HRTEM) images were recorded using a FEI Talos F200x G2 microscope working at 200 kV. Energy-dispersive X-ray spectroscopy (EDX) and elemental mapping were obtained under the STEM mode. The STEM-EDX spectrum was recorded using a super-x analysis system. The powder samples were dispersed in water with the ultrasonic treatment for 10 min and dropped onto a copper grid.

N₂ adsorption-desorption measurement was performed at -196 °C on a Quantachrome Autosorb iQ instrument to determine the specific surface area of the catalysts. Prior to the measurement, the sample was degassed under vacuum at 200 °C for 4 h. The specific surface areas were calculated using the Brunauer-Emmett-Teller (BET) method.

X-ray photoelectron spectroscopy (XPS) data of the fresh and spent samples were recorded on a Thermo Scientific K-Alpha+, employing monochromated Al K α ($h\nu = 1486.6 \text{ eV}$) as the exciting source at 12 kV and 6 mA.

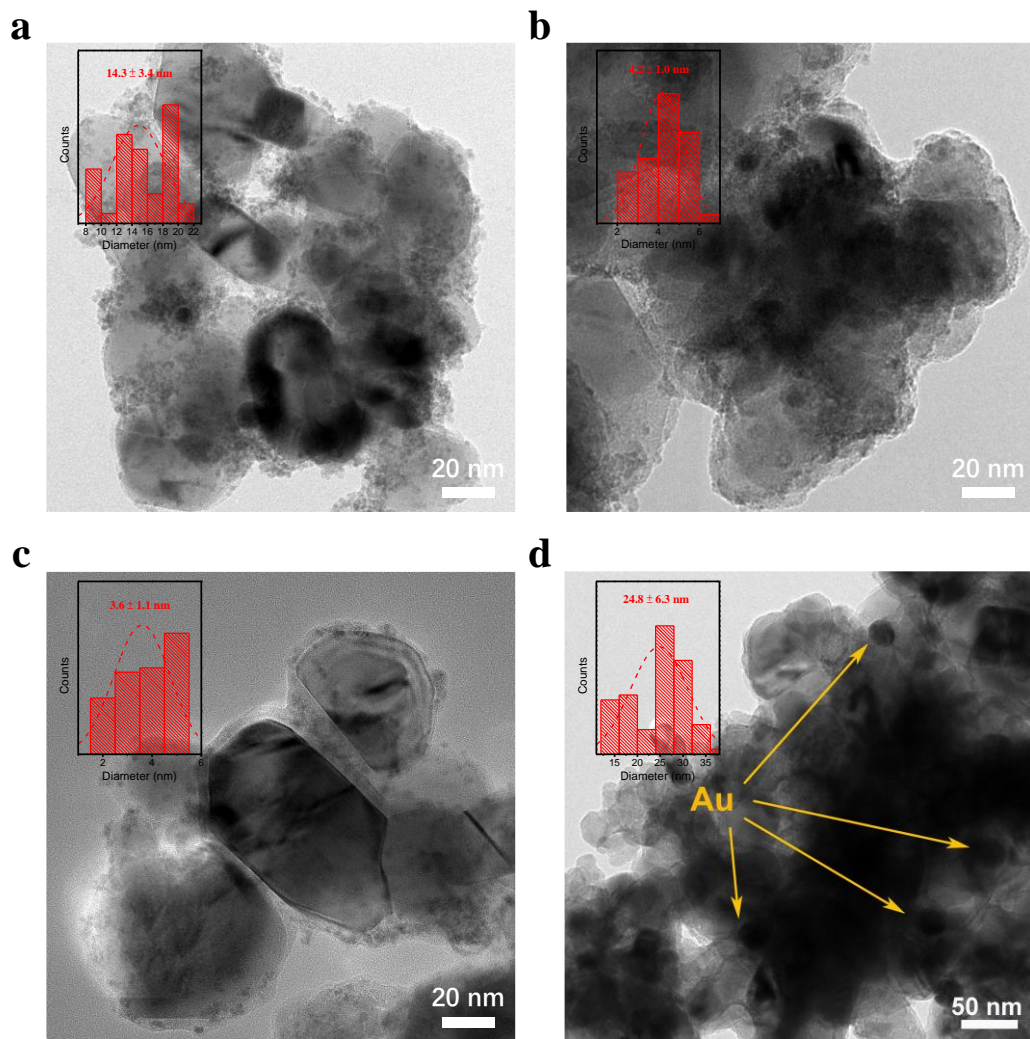


Fig. S1 TEM images of (a) Au@1Ce-RTi, (b) Au@3Ce-RTi, (c) Au@5Ce-RTi and (d) Au-RTi catalysts on the larger scale (inset was the diameter distribution of Au NPs).

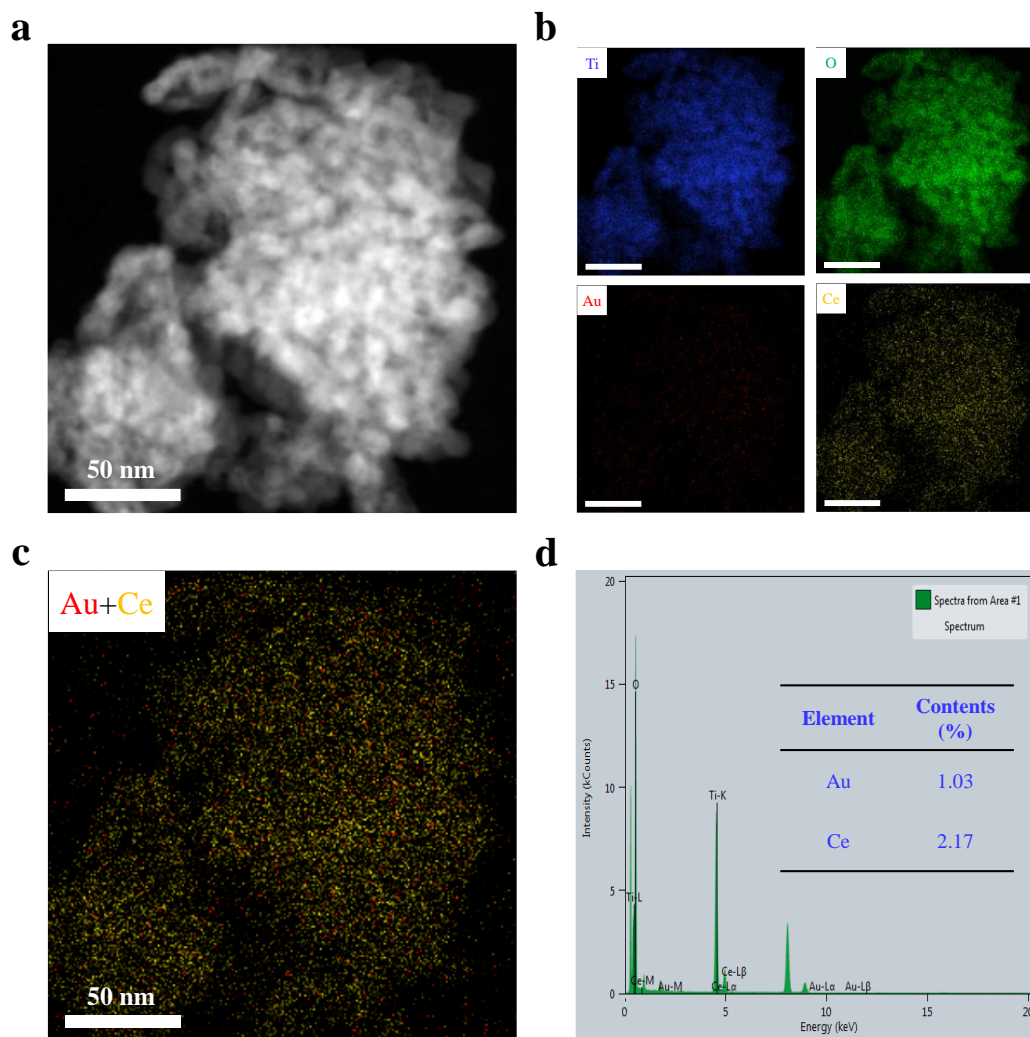


Fig. S2 (a) HAADF image and (b) EDX elemental mapping of Au@3Ce-RTi catalyst (Ti: blue, O: green, Au: red, Ce: yellow), (c) EDX elemental mapping of Au and Ce, (d) element contents of Au and Ce in the image.

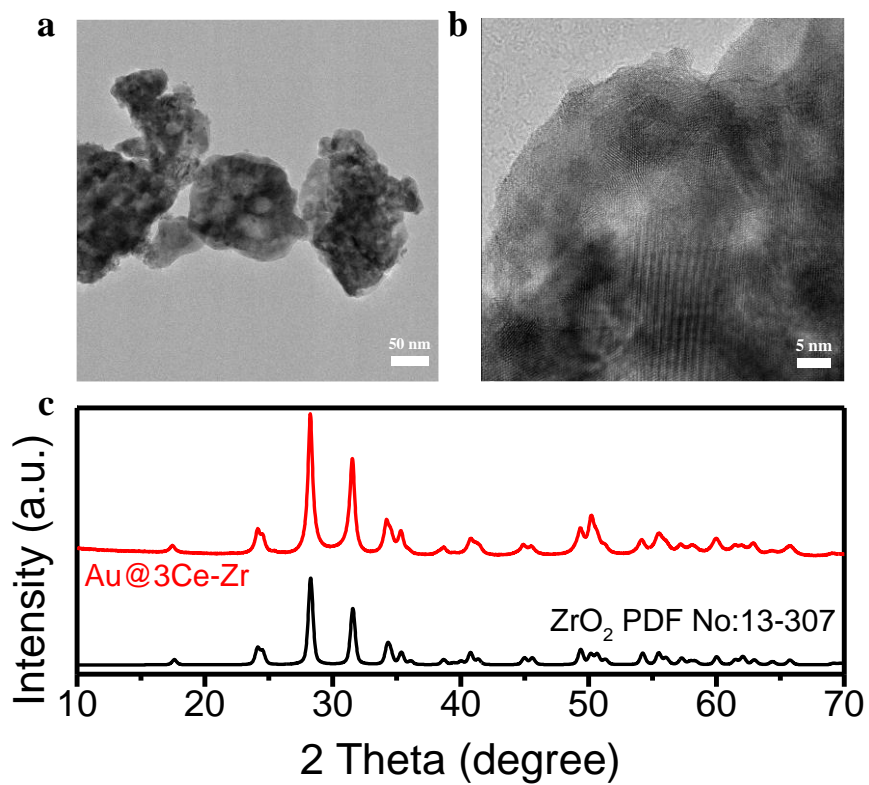


Fig. S3 (a and b) TEM and HRTEM images of Au@3Ce-Zr catalyst. (c) corresponding XRD pattern of this catalyst.

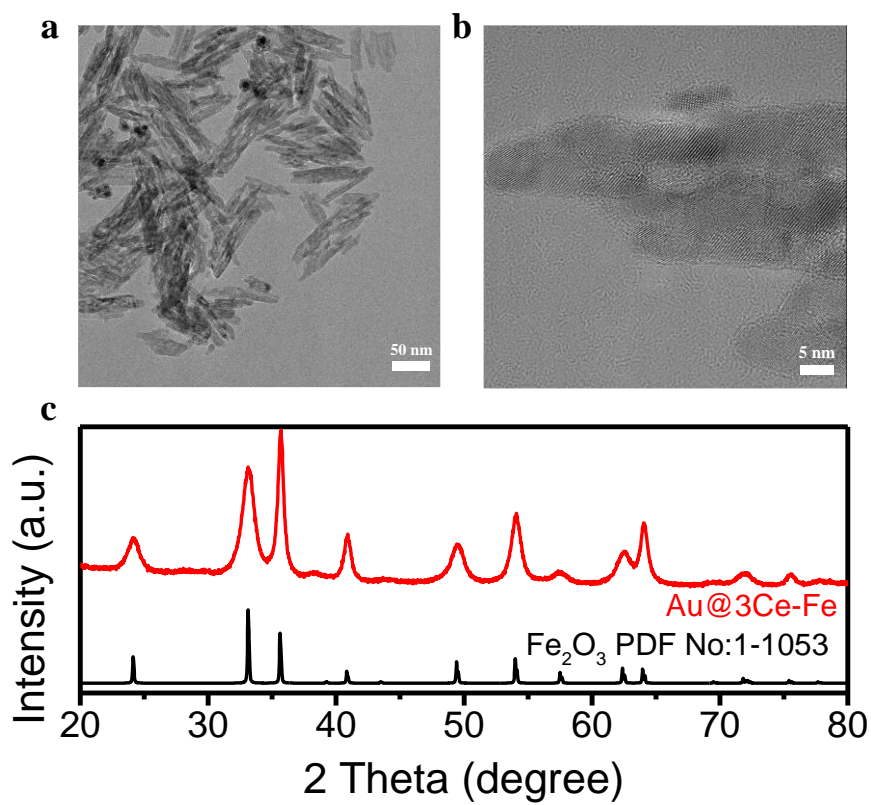


Fig. S4 (a and b) TEM and HRTEM images of Au@3Ce-Fe catalyst. (c) corresponding XRD pattern of this catalyst.

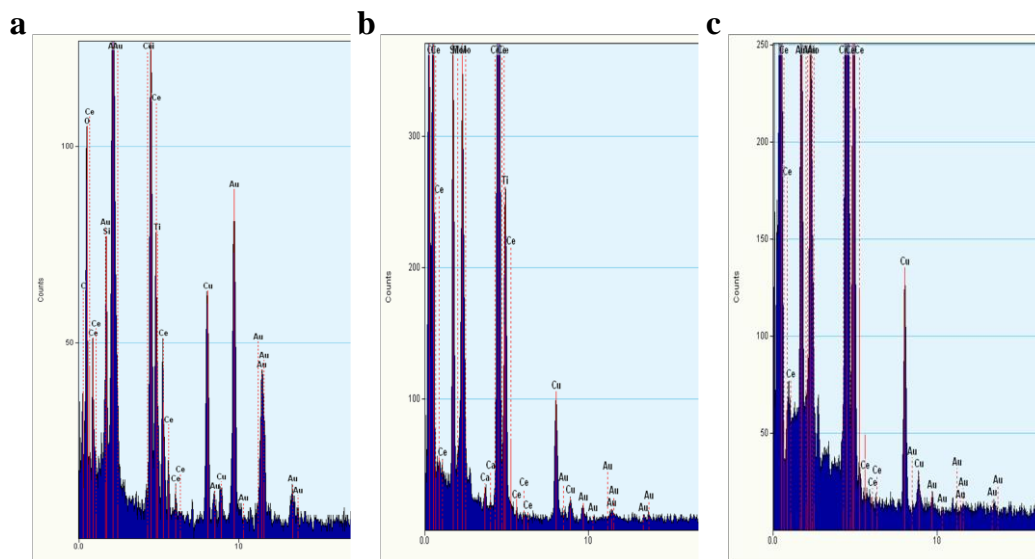


Fig. S5 The EDX spectra in TEM mode around the Au NPs over (a) Au@1Ce-RTi, (b) Au@3Ce-RTi and (c) Au@5Ce-RTi catalysts.

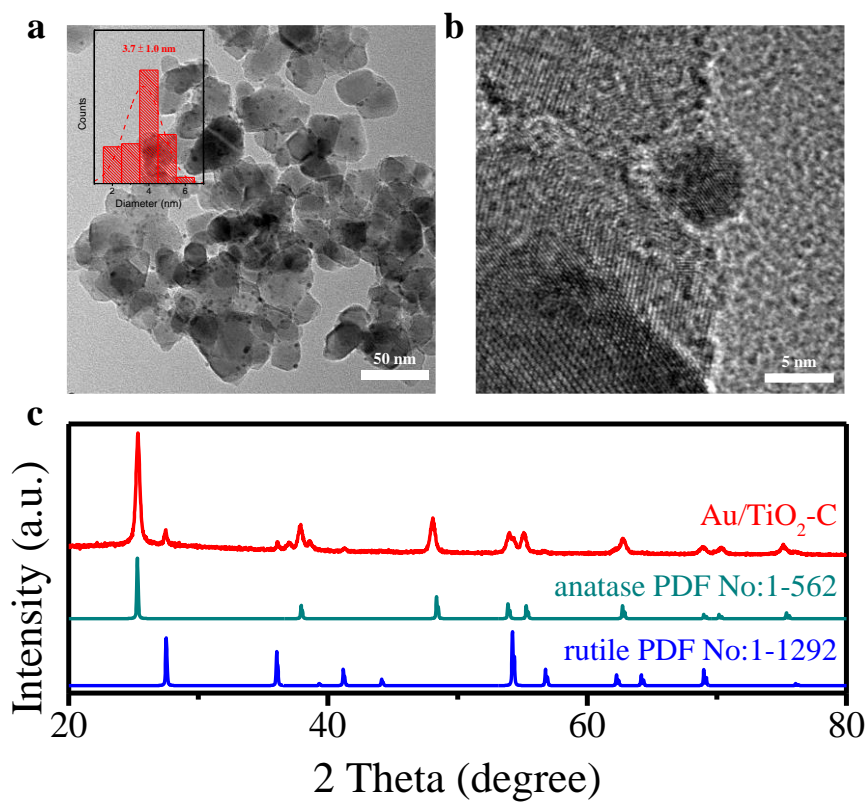


Fig. S6 (a and b) TEM and HRTEM images of the referenced commercial Au/TiO₂-C catalyst (inset was the diameter distribution of Au NPs). (c) corresponding XRD pattern of this catalyst.

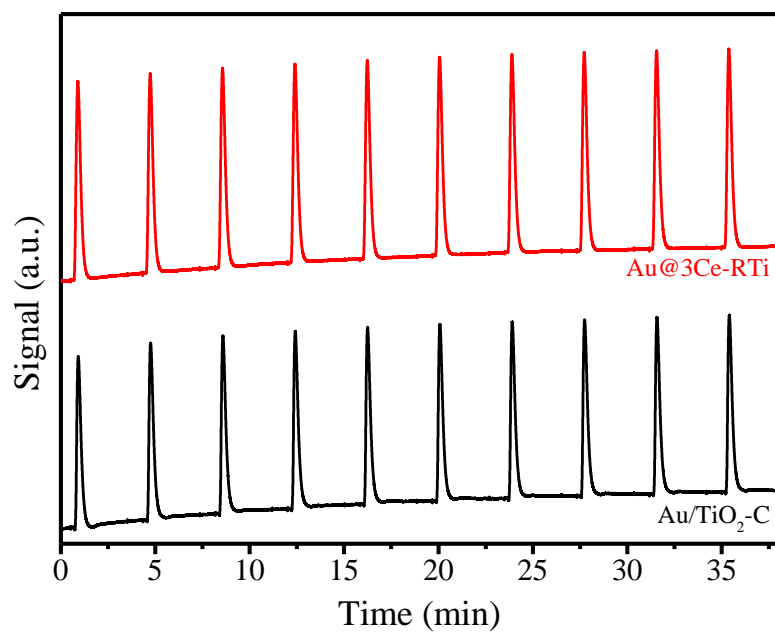


Fig. S7 CO pulse chemisorption patterns of the Au@3Ce-RTi and Au/TiO₂-C catalysts. The metallic surface area (with reference to the content of metal) were 15.26 m² g⁻¹ for Au/TiO₂-C catalyst and 9.89 m² g⁻¹ for the Au@3Ce-RTi catalyst.

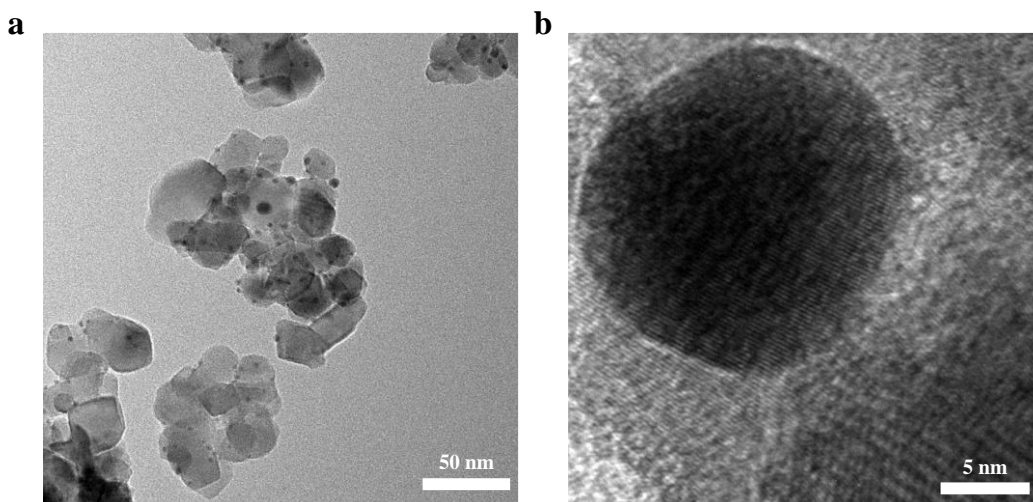


Fig. S8 (a and b) TEM and HRTEM images of Au/TiO₂-C catalyst after 100 h long-term catalytic tests.

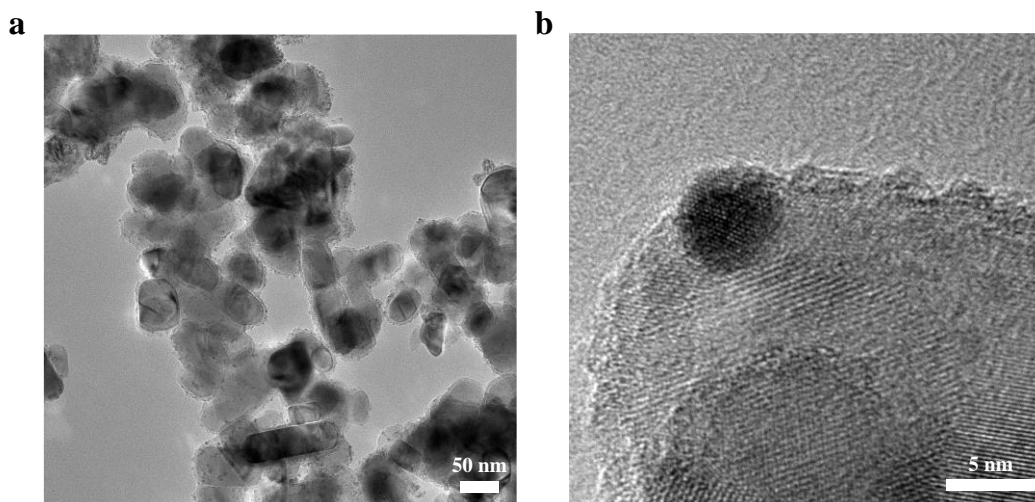


Fig. S9 (a and b) TEM and HRTEM images of Au@3Ce-RTi catalyst after 100 h long-term catalytic tests.

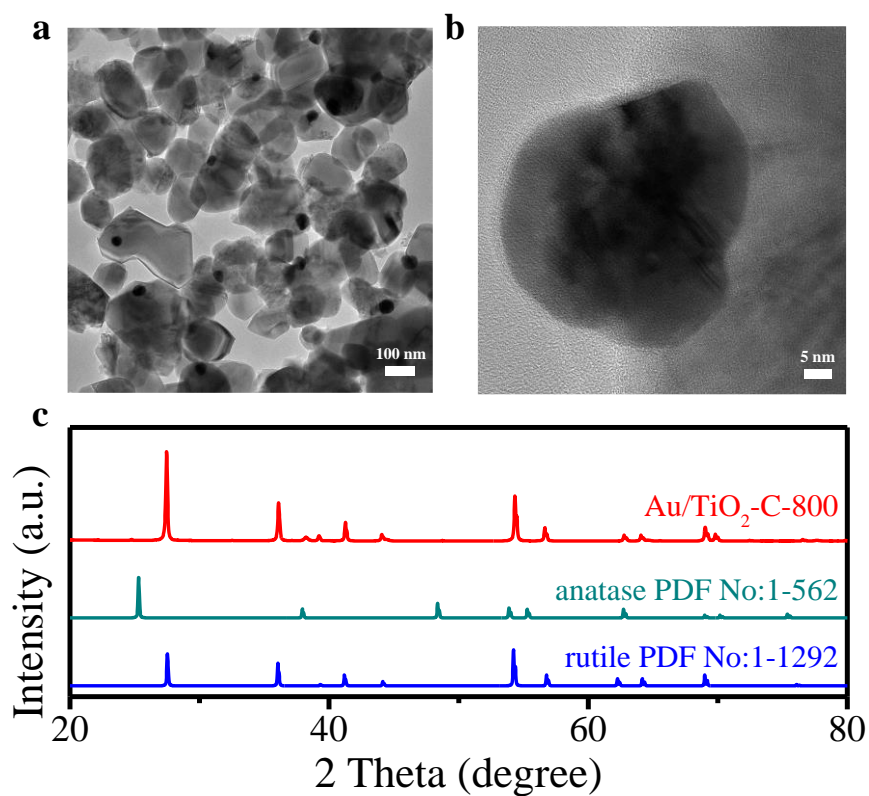


Fig. S10 (a and b) TEM and HRTEM images of Au/TiO₂-C-800 catalyst derived from once calcination treatment of Au/TiO₂-C sample at 800 °C. (c) corresponding XRD pattern of this catalysts.

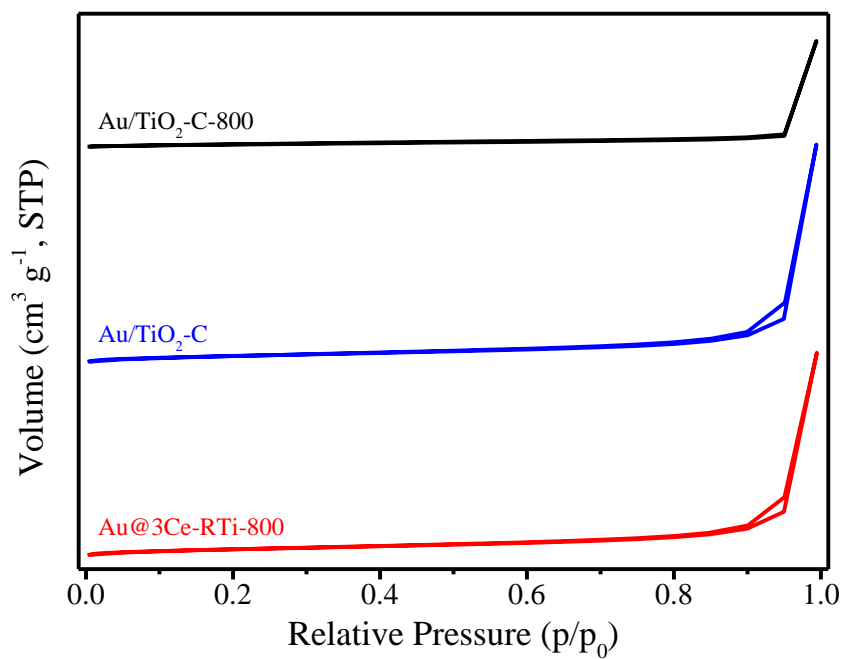


Fig. S11 N₂ adsorption-desorption isotherms of the Au/TiO₂ and Au@3Ce-RTi catalysts after calcination treatment.

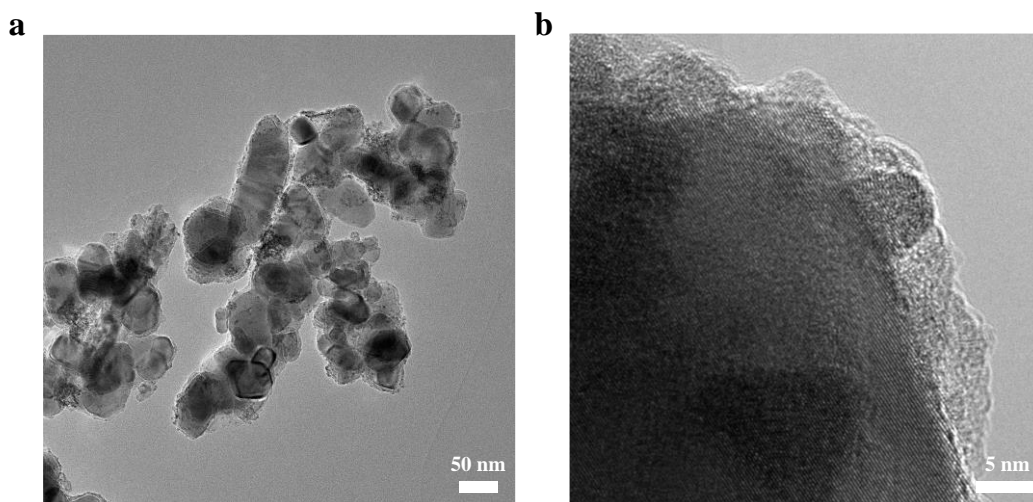


Fig. S12 (a and b) TEM and HRTEM images of Au@3Ce-RTi-800 catalyst derived from once calcination treatment of Au@3Ce-RTi sample at 800 °C.

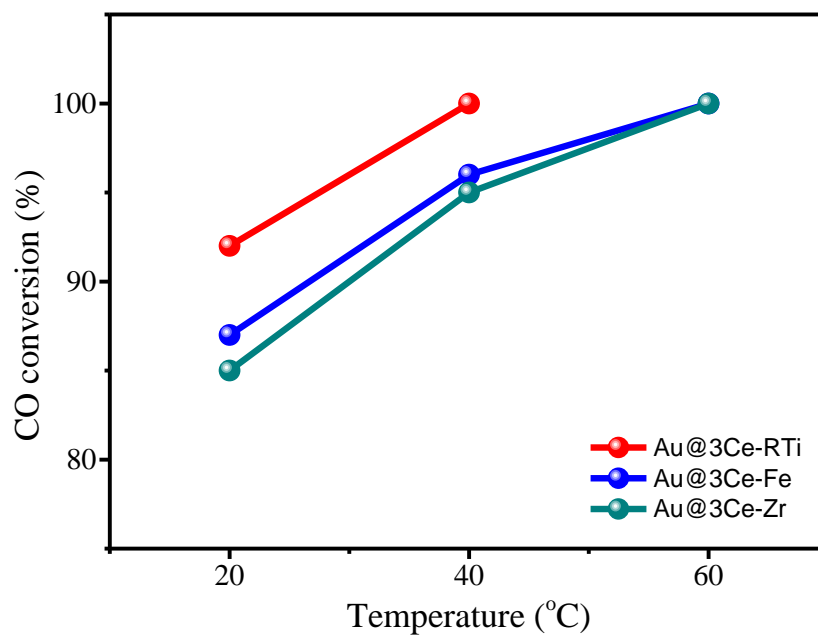


Fig. S13 The comparison of catalytic performance for CO oxidation over Au@3Ce-RTi, Au@3Ce-Zr and Au@3Ce-Fe catalysts under same condition (feed gas composition: 1.0 vol% CO, 10 vol% O₂ and balance He; GHSV = 30,000 mL g_{cat}⁻¹ h⁻¹).

Table S1. The ICP results of Au and Ce in different gold catalysts

Entry	Samples	Au loading (%)	Ce loading (%)
1	Au-RTi	1.034	—
2	Au@1Ce-RTi	0.989	0.705
3	Au@3Ce-RTi	1.025	2.149
4	Au@5Ce-RTi	1.051	3.517
5	Au@3Ce-RTi-800	1.017	2.118
6	Au/TiO ₂ -C	1.026	—
7	Au/TiO ₂ -C-800	1.013	—

Table S2. The surface area of different gold catalysts

Catalysts	Specific surface area (m ² g ⁻¹)	Total pore volume (cm ³ g ⁻¹)
Au-RTi	25.577	0.230
Au@1Ce-RTi	25.702	0.246
Au@3Ce-RTi	29.428	0.258
Au@5Ce-RTi	21.737	0.184
Au@3Ce-RTi-800	26.186	0.243
Au/TiO ₂ -C	25.713	0.249
Au/TiO ₂ -C-800	8.528	0.119

Table S3. TOF values of various gold catalysts in this work

Catalysts	CO conversion T ₂₀ ^a (%)	Au diameter ^b (nm)	TOF ^c (s ⁻¹)
Au-RTi	8	24.8	0.12
Au@1Ce-RTi	14	14.3	0.13
Au@3Ce-RTi	92	4.2	0.26
Au@5Ce-RTi	32	3.6	0.08
Au/TiO ₂ -C	90	3.7	0.22

(a) CO conversion were obtained in the condition of 1 vol% CO and 10 vol% O₂;

(b) Measured by TEM;

(c) Considering the influence of CeO_x coverage on CO adsorption over Au NPs surface, we did not use CO chemisorption content to calculate the dispersion and the number of surface active sites. The gold dispersion was calculated according to $D = 1/d_{Au}$, where d means diameter.